J. Phys. B: At. Mol. Opt. Phys. 23 (1990) 577-588. Printed in the UK

Elastic and vibrational differential cross sections for collisions of low- and intermediate-energy electrons with silane†

H Tanaka‡, L Boesten§, H Sato||, M Kimura¶#, M A Dillon¶ and D Spence¶

‡ Department of General Sciences, Sophia University, Chiyoda-ku, Tokyo, Japan 102
§ Department of Physics, Sophia University, Chiyoda-ku, Tokyo, Japan 102
|| Department of Physics, Ochanomizu University, Bunkyo-ku, Tokyo, Japan 112
¶ Argonne National Laboratory, Argonne, Illinois 60439, USA
# Department of Physics, Rice University, Houston, Texas 77251, USA

Received 17 May 1989, in final form 12 September 1989

Abstract. Absolute elastic differential cross sections for electron collisions with silane (SiH_4) have been determined for incident electron energies of 1.8, 2.15, 2.65, 3, 4, 5, 7.5, 10, 15, 20, 40 and 100 eV over a scattering angular range of 20-130°. The measured angular distributions have been found to correspond quite well with the results of approximate theories employing either a multiple scattering formalism or an optical potential.

Angular and energy distributions as well as vibrational excitation functions obtained with electrons of about 1.5-7 eV reveal the existence of a Si-H σ^* shape resonance with a maximum at around 1.8-2.2 eV in the t_2 component of the scattered electron state. As predicted by a selection rule the same resonance is found in vibrational excitation functions obtained with electrons in this energy range. A multiple scattering calculation has been used to explain details of the resonance structure.

1. Introduction

Due to its importance in the semiconductor industry, silane (SiH_4) which has a T_d symmetry, remains one of the most useful media for photochemical and discharge-induced plasmas. Modelling of plasma kinetic processes requires, as input, absolute ionisation and excitation cross sections over a range of electron energies.

Absolute differential cross sections for electron collisions with molecules of T_d symmetry also provide a crucial testing ground for various approximate solutions of the electron (e)-molecule scattering problem. These theories generally fall into two classes: the multiple scattering approximation and *ab initio* formulations in which non-local terms are replaced with analytical potentials. Examples of the latter approach include those of Jain and Thompson (1987), Jain (1987), Jain *et al* (1987) and Gianturco *et al* (1987).

The continuum multiple scattering (CMS) method, as originally formulated by Dill and Dehmer (1974), renders the e-molecule problem more tractable by subdividing it

† Work supported in part by the US Department of Energy, Office of Health and Environmental Research, under Contract W-31-109-Eng-38, Office of Basic Energy Sciences, and by Grant in Aid from the Ministry of Education, Science, and Culture, Japan.

0953-4075/90/030577+12$03.50

into separate calculations for three contiguous regions. This approach allows a simplified connection between the complex molecular field and the spherically symmetric asymptotic region. The CMS method has been applied to the e-SiH_4 elastic scattering problem by Tossel and Davenport (1984) and appears to give results comparable with those obtained with the approximate *ab initio* calculations.

Experimentally, electron collisions with SiH_4 have been investigated by various techniques. A minimum was observed in its derivative electron transmission spectrum near 2 eV by Giordan (1983) and tentatively assigned as arising from a silicon σ_π^* orbital. Sueoka and Mori (1985) measured the total elastic cross section with a retarding-potential time-of-flight apparatus and found a peak at 3.1 eV of approximate magnitude 52×10^{-16} cm^2, accompanied by a barely visible hump near 8 eV (cf Gianturco's paper). In addition, Hayashi (1987), Kurachi and Nakamura (1988), and Ohmori *et al* (1986), following Pollock's method (Pollock 1968), derived peaks in vibrational excitation functions at 2.5 eV from measured electron swarm parameters. Finally, Tronc *et al* (1989) (see also Ben Arta and Tronc 1988) have observed a broad peak at 2.1 eV in a vibrational excitation function for overlapping modes ν_1 and ν_3 recorded at a scattering angle of 30°.

In the present study we give a comprehensive set of elastic cross sections for scattering of electrons with energies of about 1.8–100 eV from silane. These are compared with a CMS calculation employing recent refinements by Kimura *et al* (1989) and Sato *et al* (1988). The 100 eV measurements are also compared with results of a calculation by Jain (1987) which utilises an optical potential to account for open inelastic channels. Also, the origin of a shape resonance with a maximum in the 1.8–2.5 eV range is discussed with reference to the theory of Andrick and Read (1971). This theory as well as the refined CMS calculation are used to elucidate the behaviour of energy and angular distributions of scattered electrons.

2. Experimental procedure

The apparatus employed in the present work has been described in detail elsewhere (Tanaka *et al* 1988). It uses crossed electron and molecular beams and the relative flow method (Srivastava *et al* 1975) for both elimination of machine-dependent factors and normalisation. The gas flow was monitored via the stagnation pressure (P), and gas beam profiles were held constant by adjusting P to obtain equal Knudsen numbers for different gases. The reference gas was He, together with the low-energy cross section set compiled by Boesten (1988). In the case of angular distribution measurements, the energy scale was calibrated by reference to the 19.37 eV resonance in He. The excitation function energy scale was calibrated by reference to the first maximum at 1.97 eV of N_2 ($v = 0 \rightarrow 1$) in an $N_2 + SiH_4$ gas mixture.

In order to minimise the deleterious effects of SiH_4 on the electron optical systems, backing pressure and instrumental resolution were reduced, and acquisition times were shortened, thus sacrificing statistical accuracy. In addition, the region above the gas jet was differentially pumped through a tube containing a cold finger. Under these conditions (resolution 40 meV) the neighbouring vibrational modes ν_1(0.1213 eV), ν_3(0.1128 eV) and ν_2(0.2712 eV), ν_4(0.2707 eV) could not be resolved and, in what follows, the overlapping bands are referred to as ν_{13} and ν_{24}.

The angular distributions of elastic scattering shown in figure 1 were normalised by reference to the He DCS measurements under the same experimental conditions

with the exception of the stagnation pressure. The measured DCS were converted into absolute cross sections by use of the standard formula

$$\sigma_{SiH_4} = \sigma_{He} \frac{I_{SiH_4} P_{He}}{I_{He} P_{SiH_4}} \tag{1}$$

where σ_{He} is the known elastic DCS of He, and I indicates the measured intensities.

Angular distributions of the vibrational excitation cross sections ν_{13} and ν_{24} as displayed by figure 6 were normalised by comparing areas under the respective peaks (± 0.05 eV from central peak) with the area under the elastic peak recorded in the same scan.

Finally, excitation functions such as those displayed in figure 5 were treated in a different manner. They were normalised channel by channel by reference to the elastic peak of SiH_4 measured under identical experimental conditions including pressure. Here, it is assumed that the transmision of the analyser lens system remains approximately constant over the small shift in energy ($\Delta E = 0.12$ or 0.27 eV). Single-channel normalisation is important because lens calculations as well as experiments show that the diameter and thus the density of the impact electron beam changes dramatically (1:25) over the excitation energy range when zoom action is obtained from a single focus-correcting voltage. If such a normalisation were not done, the peaks of the excitation functions at smaller angles would appear at about 0.4–0.5 eV higher energies compared with those shown in figure 5. Note that the papers by Ben Arta and Tronc (1988) and Tronc *et al* (1989) do not mention such corrections. Their peak in the excitation function of ν_{13} for 30° appears at an energy of about 2.1 eV.

At very low energies, normalisation of the excitation functions leads to a division by small numbers with subsequent increase in statistical fluctuations—in spite of smoothing of the measured He intensities. As a quick inspection of equation (1) and the formula for normalisation with reference to the elastic peak will show, one can measure the vibrational excitation of SiH_4 and that of He at $\Delta E = 0$ and use equation (1) directly to reduce error propagation.

3. Theoretical outline

The continuum multiple scattering (CMS) method has proven to be a successful tool for full elucidation of various experimental observations in electron-polyatomic molecule collisions. In particular, the method is useful for studying larger molecules where *ab initio* theoretical approaches are not readily applicable due partly to excessive computer time. Both the advantage and disadvantage of the CMS is the partitioning of the molecular configuration space into three regions, each with a corresponding potential: the atomic spheres (region I), the spherical region surrounding the whole molecule (region III), and the interstitial region (region II). The present modified version of the CMS (Kimura *et al* 1989) uses a more realistic SCF potential in region I, calculated by the discrete variable DV $X\alpha$ method of Averill and Ellis (1973). The molecular states of SiH_4 were calculated according to the DV $X\alpha$ method for the following nuclear geometry (Anderson *et al* 1979): bond length = 2.787 au, bond angle = 109.57°. The potential in region III of space comprises a superposition of direct and exchange electrostatic potentials plus a polarisation potential. For the polarisation coefficient we used the value $\alpha = 30.4$ found in the calculation by Jain (1987). The

scattering matrix was then constructed from wavefunctions numerically determined by matching across the boundary region.

4. Results and discussion

Elastic cross sections determined in the manner described in § 2 are given in table 1. These are plotted in figures 1(*a*)-(*c*) together with cross section curves obtained from the modified CMS calculation. The data presented here cover regions below and above the excitation threshold which for the purpose of discussion are designated ranges I and II, respectively.

4.1. Range I (1.8-5 eV)

Angular distributions obtained with electrons of 1.8-5 eV incidence energy are displayed in figure 1(*a*). The curves labelled 1.8-2.65 eV show the emergence of a prominent peak near a scattering angle of 90°. The energy dependence of this peak, as depicted in the energy distributions of figure 2, reveals a broad maximum in the 90° curve centred at about 2.2 eV. The intensity and position of the maximum change with scattering angle in such a way that its location in an integrated cross section might appear at somewhat higher energy.

The shape of the angular distribution in figure 1(*a*) recorded with 1.8 eV electrons indicates a dominant d-wave characteristic in the scattered e wave (maximum near 90° and minima near 60°, Bardsley and Read 1968). This is confirmed by the present calculation as well as those reported earlier which demonstrate a π radian change in the eigenphase sum of the T_2 scattering state with most of the amplitude and phase change occurring in the $l=2$ component. Thus, the peak in figure 2 indicates the production of a temporary negative ion (TNI, see Robin 1985) formed by the insertion of an incident electron into a low-lying antibonding valence orbital belonging to the t_2 representation. The half width of the peak is broad enough ($\sim$1 eV) and hence the lifetime short enough ($\sim 10^{-15}$ s) to eliminate Jean-Teller distortions. TNI decay to the ground state in its lowest vibrational mode must give rise to an e wave also belonging to irreducible representation t_2 (Read 1968). Although an expansion of a t_2 wavefunction into spherical harmonics will include all terms with $l \geq 1$ (Altmann and Bradley 1962) both experiment and theory show that the $l=2$ term is dominant since it provides a centrifugal barrier large enough to assure observation (Jordan and Burrow 1978).

4.2. Range II ($E \geq 7.5$ eV)

Differential cross sections obtained for electron energies above the inelastic threshold are displayed in figures 1(*b*) and (*c*). Except for the highest energy, the CMS calculations reproduce the experimental values quite well both in shape and magnitude. In figure 3 our 100 eV results are compared with those obtained from the CMS calculation and from a similar calculation by Jain (1987) employing a parameter-free optical potential. Even by varying V_{II}, the CMS calculation could not approach the experimental data. An increase in V_{II} tends to give a closer correspondence between experiment and theory at smaller scattering angles but with an increased discrepancy at larger angles due to a shift in the minimum. A similar phenomenon is observed in the case of Jain's calculation (1987) where a purely static potential yields a minimum displaced to smaller

Table 1. Elastic cross sections in units of 10^{-16} cm^2 sr^{-1} and 10^{-16} cm^2.

	E_0(eV)											
θ (deg)	1.80	2.15	2.65	3	4	5	7.5	10	15	20	40	100
10									23.473	23.480	35.644	10.110
15									21.948	19.857	17.680	4.165
20	3.352	4.243	5.166	7.407	11.221	13.490	18.709	19.985	18.028	15.426	9.891	1.684
30	2.861	4.233	5.858	6.459	11.032	12.450	17.061	15.271	10.248	7.035	2.447	0.509
40	1.870	3.058	4.818	5.587	7.980	9.524	10.870	7.998	4.657	2.708	0.734	0.277
50	1.073	2.056	3.365	3.702	5.580	6.696	6.403	4.227	1.917	0.891	0.364	0.127
60	1.080	1.575	2.477	2.723	3.423	3.994	3.467	2.091	0.699	0.423	0.255	0.0915
70	1.340	1.853	2.331	2.309	2.144	2.283	1.855	0.990	0.478	0.426	0.227	0.101
80	2.017	2.370	2.466	2.360	1.828	1.655	1.344	0.936	0.612	0.540	0.229	0.0923
90	3.064	3.058	2.686	2.670	1.525	1.524	1.490	1.334	0.750	0.519	0.276	0.0599
100	3.019	2.990	2.844	2.605	1.563	1.578	1.801	1.400	0.768	0.415	0.241	0.0268
110	2.359	2.581	2.458	2.325	1.517	1.432	1.966	1.370	0.612	0.326	0.196	0.00941
120	1.771	2.163	2.036	1.831	1.333	1.432	1.709	1.150	0.400	0.209	0.131	0.0192
130	1.458	1.806	1.861	1.729	1.475	1.552	1.521	0.892	0.244	0.147	0.0943	0.0461
Q_I	27.5	31.6	34.8	36.5	40.1	44.4	49.9	39.4	28.7	20.7	14.0 ??	4.3 ?
Q_M	29.0	30.1	29.1	28.1	24.5	25.6	24.4	15.8	11.2	8.7	2.9 ?	1.2 ?

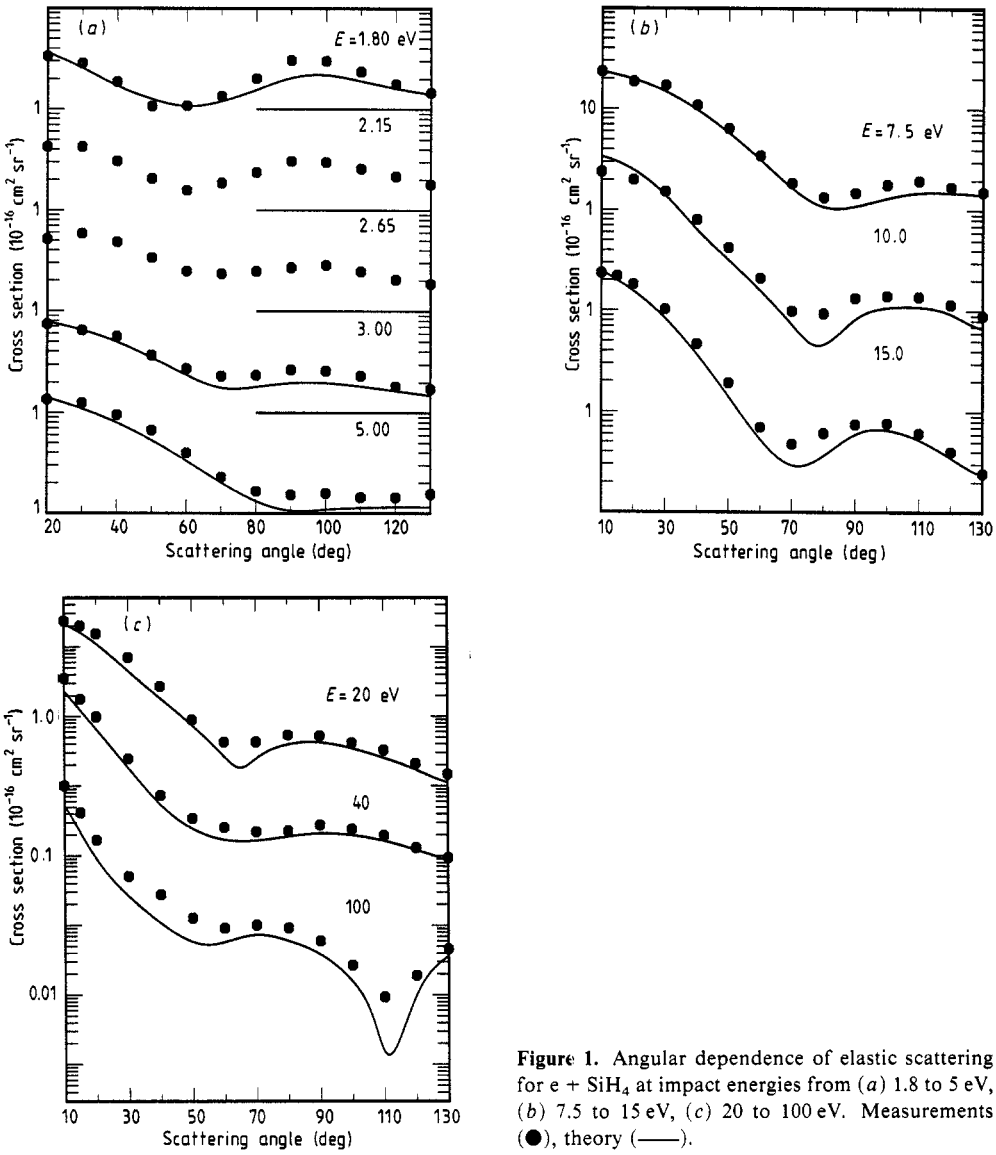

Figure 1. Angular dependence of elastic scattering for e + SiH_4 at impact energies from (*a*) 1.8 to 5 eV, (*b*) 7.5 to 15 eV, (*c*) 20 to 100 eV. Measurements (●), theory (——).

scattering angles. By adding an imaginary part to the scattering potential the location of the minimum (Jain 1987) agrees with the experimentally determined position. However, it is achieved only by underestimating the cross sections at all scattering angles.

In order to compare present results with data reported in the literature it is necessary to form integral quantities from the differential cross sections presented in table 1 and figures 1(*a*)-(*c*). The two lowest rows of table 1 include estimates of the momentum transfer cross section, shown in figure 4, and of the integrated cross sections. They were obtained with the help of a modified phaseshift fitting program (cf Tanaka *et al* 1982) using five parameters (including size) for the 1.8-5 eV range and from six to eight parameters for the higher energies. For 100 eV an artificial point gleaned from

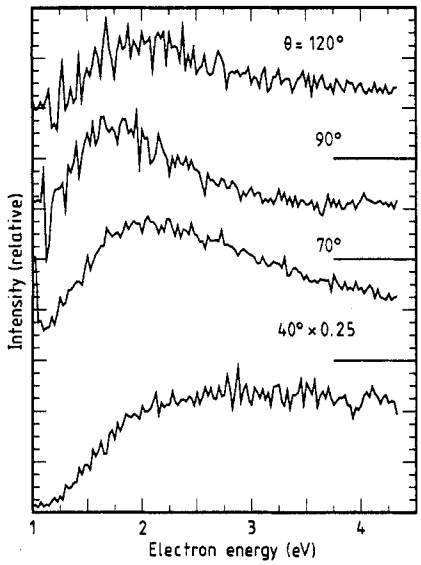

Figure 2. Energy dependence of elastic scattering for e + SiH_4 scattering at various angles. The steep rise to the left is an artifact arising from division by small numbers.

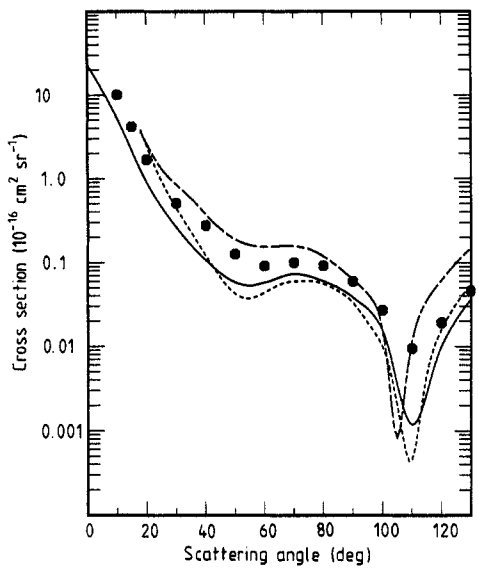

Figure 3. e + SiH_4 elastic scattering at 100 eV: experiment (●); CMS calculation (——); static potential, Jain (1987) (— — —); optical potential, Jain (1987) (· · ·).

theory was added at $\theta = 160°$, and at 40 eV a manual extrapolation was used. The fits become somewhat unreliable at higher energies, but results compared favourably with those of Hayashi (1987). Two peaks can be observed in the momentum transfer cross sections σ_M, one at around 7.5 eV which just echoes the peak in the integrated cross section σ_I, and a second one at about 2.15 eV. The latter arises from the $(1-\cos\theta)$ factor in the formula for σ_M, which stresses high angular regions, and combines with the resonance-enhanced large DCS values in this region.

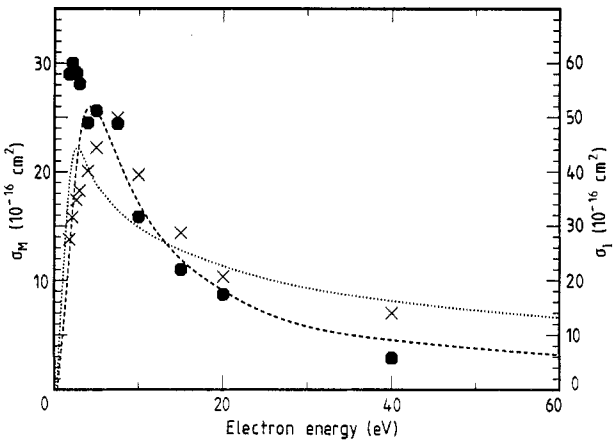

Figure 4. Integrated cross sections: present data, momentum transfer (●); present data, elastic DCS (×); Hayashi (1987), momentum transfer (——); Kurachi and Nakamura (1988), momentum transfer (· · ·).

4.3. Vibrational excitation

The T_2 resonant state responsible for the maximum in figure 2 may decay into vibrational modes other than ν_0. For an initially symmetrical state, these are given by the symmetric product of t_2, namely $(t_2 \times t_2)_s = a_1, e, t_2$ (Wong and Schulz 1975) corresponding to modes $\nu_1(a_1)$, $\nu_2(e)$, $\nu_3(t_2)$ and $\nu_4(t_2)$. Excitation functions of the two composite bands at selected scattering angles are displayed in figures 5(*a*) and (*b*). The energy distributions in both figures exhibit similar, complicated behaviour. The resonance appears as a broad peak in the excitation function at 120°, centred at about 1.8-2.2 eV. At 40°

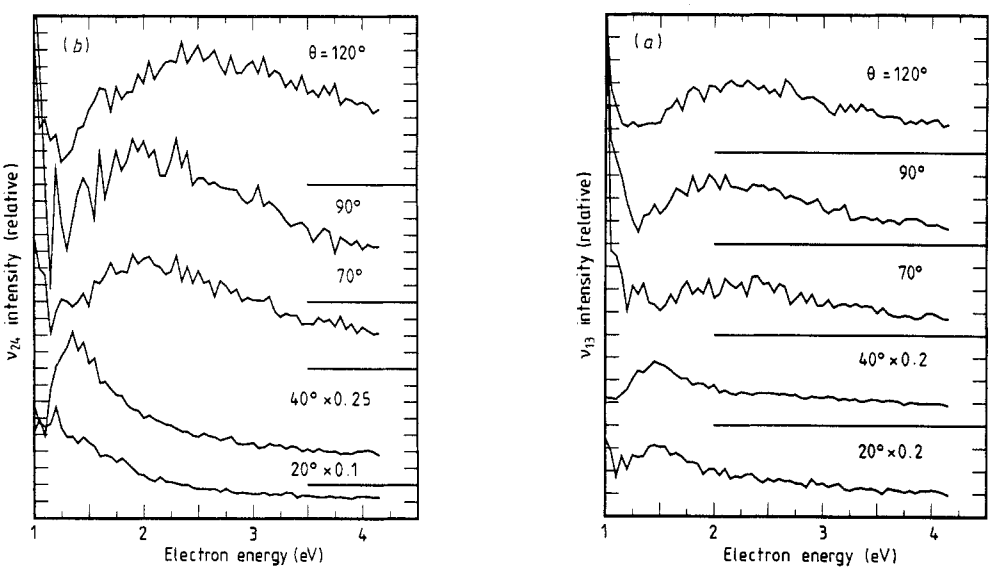

Figure 5. Excitation functions for the (*a*) ν_{13} and (*b*) ν_{24} mode in SiH_4 at various scattering angles from 20° to 120°. The steep rise to the left is an artifact arising from division by small numbers.

the peak has narrowed considerably and is shifted by about 0.5 eV to lower energy. Angular distributions for both composite peaks recorded at projectile electron energies of 2.15 and 5 eV are presented in figure 6 together with the CMS results. The distribution curves for both ν_{13} and ν_{24} excitation show a series of irregular features rather than the simple behaviour exhibited in the elastic scattering curves displayed in figure 1(*a*).

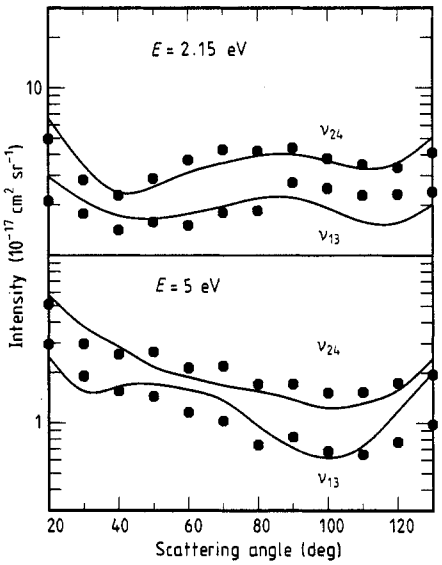

Figure 6. Angular dependence of scattering for ν_{13} and ν_{24} excitations at 2.15 and 5 eV impact energy. The full curves are the theoretical calculations.

Calculations simulating the 2.15 eV experiments of figure 6 are plotted in figure 7. The calculated curves show that (i) the infrared active modes ν_3 and ν_4 depend similarly on scattering angle, exhibiting a strong isotropic component; (ii) modes ν_1 and ν_2 also bear a strong resemblance, exhibiting a distinct maximum near a scattering angle of 90°, and (iii) the two sets of curves are completely dissimilar. The summed intensities ν_{13} and ν_{24} plotted in figure 6 show qualitative correspondence with experimental data. Hence, the irregular features in the data displayed in figure 6 are largely due to a superposition of curves with very different shapes.

The dissimilar angular distributions attributable to modes ν_1 and ν_2 in comparison with ν_3 and ν_4 are readily explained in terms of simple group theoretical constraints, which require that the electron wave (e wave) in each exit channel belongs to an irreducible representation satisfying the relationship: (mode representation) × (e-wave representation) = t_2 (Andrick and Read 1971). This operation yields for each vibrational mode the e-wave species indicated in brackets: $\nu_1(t_2)$, $\nu_2(t_2, t_1)$, and ν_3, $\nu_4(a_1, e, t_2, t_1)$. The lowest harmonics, P_m^l, for the e wave in the ν_1 and ν_2 exit channels are the same, $l = 1, 2$; $m = -1, \ldots, 0, \ldots +1$ (Altmann and Bradley 1962). On the other hand, the presence of an $l = 0$ term (a_1) leads to an isotropic appearance in the angular distributions of ν_3 and ν_4 scattering.

Excitation functions calculated at a scattering angle of 90° for the four vibrational modes are displayed in figure 8(*a*) together with composite intensities ν_{13} and ν_{24}. The calculation shows that the maximum at about 1.85 eV in the ν_{13} and ν_{24} curves

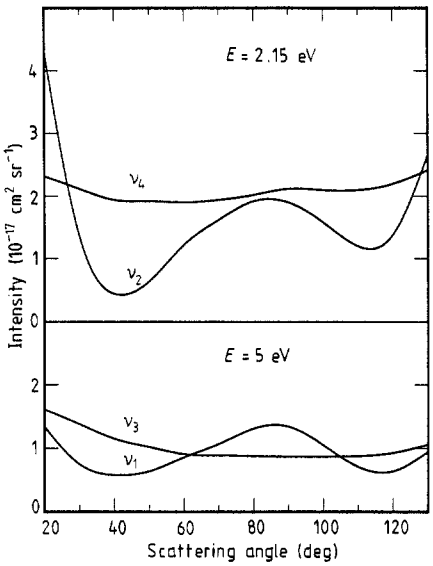

Figure 7. Calculated angular distributions for ν_1, ν_2, ν_3 and ν_4 excitations at impact energies of 2.15 and 5 eV.

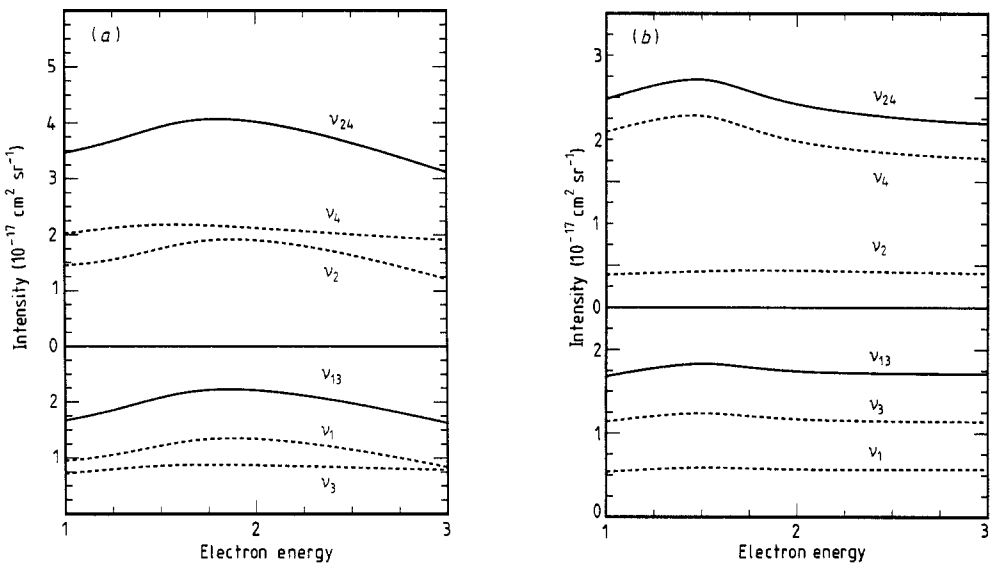

Figure 8. Calculated excitation functions for ν_1, ν_2, ν_3 and ν_4 modes at a scattering angle of (*a*) 90° and (*b*) 40°.

derives primarily from maxima in the ν_1 and ν_2 excitation functions. The same calculation for scattering at 40°, presented in figure 8(*b*), reveals a clearly narrower peak that has shifted to about 1.5 eV and now resides in modes ν_3 and ν_4. Hence, the calculated energy distributions in figures 8(*a*) and 8(*b*) account well for the shift of peak and the alteration of shape depicted in figures 5(*a*) and (*b*).

5. Conclusion

We have presented a survey of elastic cross sections for e-SiH_4 scattering over the first 100 eV incident electron energy for the purpose of aiding collision-theoretical developments as well as to implement plasma simulations. Comparison with theory demonstrates the feasibility of providing elastic collision input data in the future by computation alone.

We have also investigated the behaviour of the expected shape resonance in the neighbourhood of 2 eV. The angular trend indicates a predominant d-wave character which is consistent with electron ejection from a t_2 orbital of a short lived TNI. This particular low-lying valence orbital has already been anticipated by the observation of a transition to a mixed Rydberg-valence state of species T_2 in the electronic spectrum of SiH_4 (Tronc *et al* 1989, Ben Arta and Tronc 1988, Larrieu *et al* 1988, Dillon *et al* 1985). Finally, we have shown that it may be necessary to rely on a calculation in order to understand the complicated angular distributions and excitation functions associated with overlapping vibrational bands.

Acknowledgment

This work was supported in part by the US Department of Energy, Office of Health and Environmental Research, under Contract W-31-109-Eng-38, Office of Basic Energy Sciences, and by Grant in Aid from the Ministry of Education, Science, and Culture, Japan.

References

Altmann S L and Bradley C J 1962 *Phil. Trans. R. Soc.* A **255** 199
Anderson P R, Ellis D E and Ratner M A 1979 *Chem. Phys.* **41** 209
Andrick D and Read F H 1971 *J. Phys. B: At. Mol. Phys.* **4** 389
Averill F W and Ellis D E 1973 *J. Chem. Phys.* **59** 6412
Bardsley J N and Read F H 1968 *Chem. Phys. Lett.* **2** 333
Ben Arta M and Tronc M 1988 *J. Chim. Phys.* **85** 889
Boesten L 1988 *43rd Ann. Meeting of the Phys. Soc. Japan (Koriyama)* 31a G2 9, unpublished
Dill D and Dehmer J L 1974 *J. Chem. Phys.* **61** 692
Dillon M A, Wang R-G, Wang Z-W and Spence D 1985 *J. Chem. Phys.* **82** 2909
Gianturco F A, Pantano L C and Scialla S 1987 *Phys. Rev.* A **36** 557
Giordan J C 1983 *J. Am. Chem. Soc.* **105** 6544
Hayashi M 1987 *Swarm Studies and Inelastic Electron-Molecule Collisions* ed L C Pitchford *et al* (Berlin: Springer) p 167
Jain A 1987 *J. Chem. Phys.* **86** 1289
Jain A and Thompson D G 1987 *J. Phys. B: At. Mol. Phys.* **20** 2861
Jain A K, Tripathi A N and Jain A 1987 *J. Phys. B: At. Mol. Phys.* **20** L389
Jordan K D and Burrow P D 1978 *Acc. Chem. Res.* **11** 341
Kimura M, Sato H and Fujima K 1989 unpublished
Kurachi M and Nakamura Y 1988 private communication
Larrieu C, Liotard D, Chaillet M and Dargelos A 1988 *J. Chem. Phys.* **88** 3848
Ohmori Y, Shimozuma M and Tagashira H 1986 *J. Phys. D: Appl. Phys.* **19** 1029
Pollock W J 1968 *Trans. Faraday Soc.* **64** 2919
Read F H 1968 *J. Phys. B: At. Mol. Phys.* **1** 893
Robin M B 1985 *Higher Excited States of Polyatomic Molecules* vol III (New York: Academic) p 54ff
Sato H, Kimura M and Fujima K 1988 *Chem. Phys. Lett.* **145** 21

Srivastava S K, Chutjian A and Trajmar S 1975 *J. Chem. Phys.* **63** 2659
Sueoka O and Mori S 1985 *At. Coll. Res. Japan* **11** 19
Tanaka H *et al* 1982 *J. Phys. B: At. Mol. Phys.* **15** 3305
Tanaka H, Boesten L, Matsunaga D and Kudo T 1988 *J. Phys. B: At. Mol. Opt. Phys.* **21** 1255
Tossel J A and Davenport J W 1984 *J. Chem. Phys.* **80** 813
Tronc M, Hitchcock A and Edward F 1989 *J. Phys. B: At. Mol. Opt. Phys.* **22** L207
Wong S F and Schulz G J 1975 *Phys. Rev. Lett.* **35** 1429